Performance of GFDM over Frequency-Selective Channels

Bruno M. Alves
Inatel
Sta. Rita Sapucaí - Brazil
alves.bm@gmail.com

Luciano L. Mendes
Inatel
Sta. Rita Sapucaí - Brazil
luciano@inatel.br

Dayan A. Guimarães
Inatel
Sta. Rita Sapucaí - Brazil
dayan@inatel.br

Ivan S. Gaspar
TU-Dresden
Dresden - Germany
ivan.gaspar@ifn.et.tu-dresden.de

***Abstract*— Cognitive Radio (CR) networks are able to establish communication using vacant channels reserved for primary users without interfering in the communication of the incumbents. In order to achieve this goal, CR must reduce out-of-band transmissions to avoid interference in adjacent channels. Usually, broadband digital communication standards that employ Cognitive engines for opportunistic spectrum allocation use OFDM as aerial interface. However, a technique called General Frequency Division Multiplexing (GFDM) has spectral characteristics that are more suitable for CR networks. The aim of this paper is to evaluate the performance of this technique over frequency-selective channels and compare it with OFDM. This comparison is made considering that GFDM and OFDM symbols present the same subcarrier separation. The simulation results shows that OFDM and GFDM present similar behavior under selective channels.**

***Index Terms*— GFDM, Frequency-Selective Channel,Performance.**

I. Introduction

The demand for high data rate in mobile communication systems has severely increased in the last years [1]. The opportunistic utilization of white spaces [2] is a solution that can be used to attend this demand, mainly in the UHF (Ultra High Frequency) bands [3] after the ATSO (Analog Television Switch-Off) [4]. Several countries are planning the ATSO and they consider reorganizing the allocation of Digital Television channels in order to release part of the UHF spectrum for mobile communication. This available spectrum, which is known as digital dividend [5], can be efficiently used by the CR (Cognitive Radio) technology [6]. In a CR network, radio terminals can sense the spectrum environment to detect white spaces, establishing the communication link in a vacant channel. The radio terminals keep sensing the spectrum and, if a primary user is detected, they change their operation frequency to occupy other white space, avoiding interferences to the primary user. The CR concept was proposed by Joseph Mitola III in 1999 [7] and it is being considered for the next generations of digital wireless communication standards, such as IEEE 802.22 [8], IEEE 802.16h [9], IEEE 802.11af [10] and LTE Advanced [11].

Interference from opportunistic users in primary users is a key issue for the CR technology. Signals from CR terminals cannot reduce the quality of service of primary users. Besides spectrum sensing techniques [12] [13] [14], which plays an important role to avoid interference in the primary users, the digital modulation scheme is a very important issue in this context. Most of modern digital communication standards use OFDM (Orthogonal Frequency Division Multiplexing) [15] as the air interface, because of its flexibility and robustness in frequency selective channels. Nevertheless, OFDM presents some drawbacks that affect its application specially in CR systems. Among these drawbacks there are the high out-of-band emission [16] and the high PAPR (Peak-to-Average Power Ratio) [17]. Out-of-band emissions are caused by the rectangular pulse shape of the filter used in the transmitter and the high PAPR is caused by the random sum of several in phase subcarriers. There are several papers in the literature proposing solutions to reduce the PAPR [17] [18] [19] [20] and the out-of-band-emissions; please see [21] and references therein.

In [22] the authors present a multicarrier transmission technique that is more suitable for CR operation because it reduces the out-of-band emissions and allows for the control of the PAPR. This technique is called GFDM (Generalized Frequency Division Multiplexing) [22] [23] [24] [25], which can be seen as a generalization of OFDM [26]. The main difference between GFDM and OFDM is that GFDM transmits $M\dot{K}$ data symbols per frame using M time slots with K subcarriers, where each data symbol is represented by a pulse shape $g(t)$. OFDM transmits K data symbols using one time slot with K subcarriers, where each symbol is represented by a rectangular pulse shape. It means that GFDM can model the spectrum shape by choosing the appropriate pulse shape $g(t)$. Moreover, the frequency spacing between the subcarriers is more flexible in GFDM than in OFDM, and the low out-of-band emission in GFDM allows for a higher flexibility for spectrum fragmentation.

GFDM can achieve higher spectrum efficiency because it does not need to use virtual subcarriers to avoid adjacent channel interference and because it reduces the ratio between the guard time interval and the total frame duration. The main drawbacks of GFDM are ICI (Intercarrier Interference) [27] and higher complexity. However, efforts are being made to reduce the complexity of the system and to obtain models that are suitable for hardware implementation [23]. Additionally, ICI-cancelling techniques can increase the performance of GFDM. In fact, DSIC (Double Sided ICI Cancelling) [28]

can reduce the BER (Bit Error Rate) of GFDM in AWGN (Additive White Gaussian Noise) channels to the same BER level achieved by OFDM.

The aim of this paper is to present the analysis of the performance of GFDM system in frequency-selective channels. Three types of receivers are considered: ZFR (Zero Forcing Receiver), MFR (Matched Filter Receiver) and Matched Filter Receiver with DSIC (MFR-DSIC). All results are compared with the performance of an OFDM system in the same conditions. All simulation results that have been obtained using Matlab are compared with theoretical ones.

The rest of the paper is organized as follows: Section II presents the generation of GFDM symbols, whereas Section III presents three techniques used to recover the transmitted information. Section IV contains the performance analysis of GFDM considering AWGN and frequency-selective channels and Section V concludes the paper.

II. Generation of the GFDM Signal

GFDM is a flexible multicarrier modulation scheme that has been introduced by Fettweis et al. [22] and has interesting features for CR applications. Figure 1 depicts the block diagram of the GFDM transmitter.

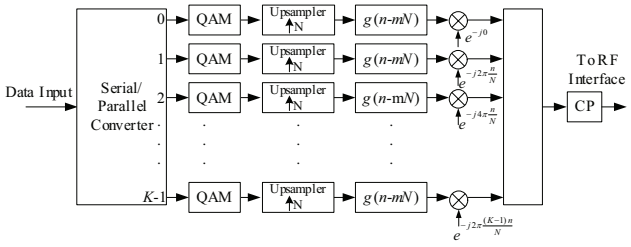

Fig. 1. Block diagram of the GFDM transmitter.

The input bits are converted into K data streams that feed K independent J-QAM mappers. Each mapper converts a block of $\log_2(J)$ bits into a data symbol to be transmitted by K different subcarriers. Since the mappers are independent, different constellation orders can be used in each stream, allowing for dynamic mapping according to the channel conditions for each subcarrier. In a GFDM, M data symbols are transmitted in the same subcarrier using M signalling windows. The data symbols are organized in a GFDM frame as follows

$$\mathbf{S} = \begin{bmatrix} s_{0,0} & s_{0,1} & s_{0,2} & \cdots & s_{0,M-1} \\ s_{1,0} & s_{1,1} & s_{1,2} & \cdots & s_{1,M-1} \\ s_{2,0} & s_{2,1} & s_{1,2} & \cdots & s_{2,M-1} \\ \vdots & \vdots & \vdots & \ddots & \vdots \\ s_{K-1,0} & s_{K-1,1} & s_{K-1,2} & \cdots & s_{K-1,M-1} \end{bmatrix}, \quad (1)$$

where the k^{th} row represents the symbols transmitted in the k^{th} subcarrier and the m^{th} column represents the symbols transmitted in the m^{th} signalling window.

Each data symbol $s_{k,m}$, $k = 0, 1, 2, \ldots, K-1$ and $m = 0, 1, 2, \ldots, M-1$, is upsampled by zero-padding $N-1$ null samples, resulting in a sequence

$$s_{k,m}(n) = s_{k,m}\delta(n - mN), \ n = 0, 1...MN-1. \quad (2)$$

This sequence is applied to a transmit filter with impulse response given by $g(n)$ with length $L = NM$. If conventional linear convolution is used, the guard time interval between the GFDM frames should be larger than the channel delay spread plus the transmit spreading in order to avoid IFI (Inter Frame Interference). Such a large guard time interval would be a considerable drawback, causing throughput reduction, leading to a poor spectrum efficiency. However, this problem can be easily avoided by a technique called tail-biting [22], which can be made by circular convolution.

The transmission filter must be properly chosen to avoid ISI (Inter Symbol Interference) and ICI (Inter Carrier Interference). Since $g(n)$ is crucial to implement the GFDM transmitter, more details about it will also be presented in the next subsection.

After pulse shaping, each independent signal is up-converted using a complex subcarrier defined by

$$p_k(n) = e^{-j2\pi\frac{k}{N}n}. \quad (3)$$

The K modulated subcarrriers are added to form the GFDM frame

$$x(n) = \sum_{m=0}^{M-1}\sum_{k=0}^{K-1} s_{k,m}\cdot\delta(n-mN) \circledast g(n-mN)\cdot p_k(n), \quad (4)$$

where $\circledast$ denotes a circular convolution.

Finally, a cyclic prefix (CP) is added to the GFDM frame to avoid IFI. Another important advantage of GFDM over OFDM is that only one CP is necessary for the entire GFDM frame, while OFDM requires one CP for each time slot. It means that the overhead caused by CP in GFDM is considerably smaller than the overhead caused by the CP in OFDM.

A. GFDM Pulse Shaping

The impulse response of the transmit filter must have MN samples to represent M different symbols in each subcarrier [22]. The impulse response must be circularly shifted by N samples in each time slot [23]. The response for the m-th time slot of an arbitrary subcarrier can be written as

$$g_m(n) = g(< n - mN >_{MN-1}) \quad (5)$$

where $< \cdot >_N$ denotes a modulo N operation. It is important to notice that $N \geq K$ to avoid alising [22].

Figure 2 shows the impulse responses of a system considering $M = 3$, $K = 8$ and $N = 24$. The transmit and receive filters are root raised cosine filters with roll-off 0.5.

The transmit filter introduces ICI among the subcarriers, which may increase the BER at the receiver side. However, if the transmit filter is properly chosen, the ICI is mostly limited to the adjacent subcarriers, as shown in Figure 3.

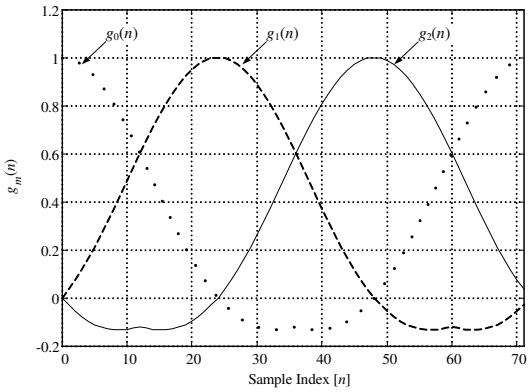

Fig. 2. Impulse response of the transmit filter considering a raised cosine with roll-off 0.5, $M = 3$, $K = 8$ and $N = 24$.

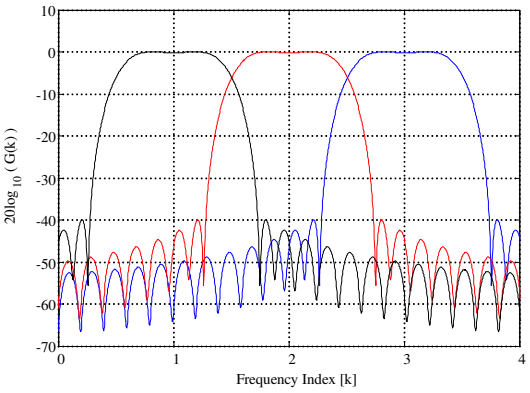

Fig. 3. Transmit filter frequency response for three adjacent subcarriers.

B. Matrix Representation

Equation (4) can be written as the matrix product between a transmission matrix $\mathbf{A}$ and a data vector $\mathbf{s}$ [22], i. e.

$$\mathbf{x} = \mathbf{A}\mathbf{s}; \tag{6}$$

Matrix $\mathbf{A}$, which has order $KM \times NM$ contains all circularly shifted impulse responses of the transmit filter modulated by all subcarriers and the data vector $\mathbf{s}$, which has order $NM \times 1$ contains all symbols transmitted in the GFDM frame.

III. Reception of GFDM Signal

Figure 4 shows the basic block diagram of a GFDM receiver. The signal from the antenna is down-converted to baseband and sampled, resulting in the discrete received signal $r_{CP}(n)$. In this paper a time-invariant multipath channel with impulse response $h(n)$ has been considered, leading to

$$r_{CP}(n) = x_{CP}(n) * h(n) + w(n) \tag{7}$$

where $x_{CP}(n)$ is the transmitted signal with CP and $w(n)$ is a sequence of gaussian noise samples with zero mean and variance σ_n^2.

The received signal is used for synchronization and for estimation of the channel impulse response. Subsequently, the

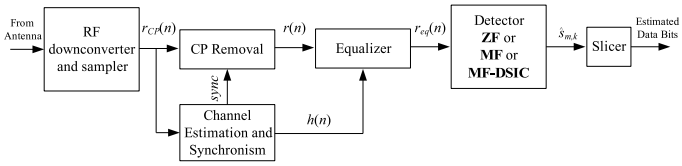

Fig. 4. Basic block diagram of an GFDM receiver.

CP is removed. It is assumed that the CP length is larger than the maximum channel delay spread, which means that there is no IFI between successive GFDM frames. Afterwards the signal must be equalized to compensate for the influence of the channel frequency response in the received signal. The channel frequency response can be considered flat for each subcarrier if K is large enough to make the subcarriers bandwidth smaller than the channel coherence bandwidth. In this case, the received signal can be equalized in the frequency domain using a Zero-forcing equalizer with a single tap per subcarrier. Assuming that the receiver is able to estimate the channel impulse response, the equalized signal can be written as

$$r_{eq}(n) = \text{IFFT}\left\{\frac{\text{FFT}\left[r(n)\right]}{\text{FFT}\left[h(n)\right]}\right\} \tag{8}$$

where FFT$(\cdot)$ is the Fast Fourier Transform and IFFT$(\cdot)$ is the Inverse Fast Fourier Transform.

The equalized signal is applied to a detector. Three different approaches are investigated in this paper: Zero-forcing (ZF), Matched Filter (MF) and Matched Filter with DSIC (MF-DSIC). After detection, the Slicer uses the recovered symbols $\hat{s}_{k,m}$ to estimate the data bits.The next subsections present these three detection processes.

A. Zero-forcing Receiver

The matrix representation of the GFDM signal in (6) allows one to conclude that the data symbols can be estimated by the ZF receiver as

$$\hat{\mathbf{s}}_{\text{ZF}} = \mathbf{A}^{-1}\mathbf{r}_{eq}, \tag{9}$$

where $\mathbf{A}^{-1}$ is the inverse of matrix $\mathbf{A}$ and $\mathbf{r}_{eq}$ is the received vector after equalization.

It is important to notice that matrix $\mathbf{A}$ has order $KM \times NM$, which means that $\mathbf{A}$ is not necessarily square. Therefore, the inversion operation is not always suitable for this matrix. When $\mathbf{A}$ is not square, it is possible to use the pseudoinverse matrix of $\mathbf{A}$, which is defined by

$$\mathbf{A}^{+} = \mathbf{A}^{H}\left(\mathbf{A}\mathbf{A}^{H}\right)^{-1}, \tag{10}$$

where $\mathbf{A}^{H}$ is the Hermitian matrix of A. Notice that $\mathbf{A}^{+}\mathbf{A} = \mathbf{I}_{KM}$, where $\mathbf{I}_{KM}$ is the identity matrix with dimension KM.

The zero-forcing receiver is capable of completely removing the ICI resulted from the non-orthogonality between the subcarriers. However, since $\mathbf{A}^{+}$ may have high values, this procedure can enhance the influence of the noise in the detected symbols, which increases the BER.

B. Matched Filter Receiver

Other possible detector is the matched filter, which is depicted in Figure 5. In this case, the data symbols transmitted in each subcarrier are detected using a matched filter. The equalized received signal is multiplied by the complex conjugate of the desired subcarrier. The resultant signal feeds the receive filter with impulse response $f_m(n) = g(< -n+mN >_{NM-1})$ that matches the transmit filter of the m-th time slot. This filtering procedure is also implemented by circular convolution [22]. The estimated received symbol $\hat{s}_{k,m}$ are obtained by sampling the output of the filter at $n = mN$.

The matched filter reception procedure can be written as

$$\hat{\mathbf{s}}_{\text{MF}} = \mathbf{A}^H \mathbf{r}_{\text{eq}} \tag{11}$$

where $\hat{\mathbf{s}}_{\text{MF}}$ is a vector containing the MK detected symbols.

The advantage of the MFR over the ZFR is that the first does not cause noise enhancement. However, the MFR is not able to eliminate the ICI caused by the non-orthogonality between the subcarriers.

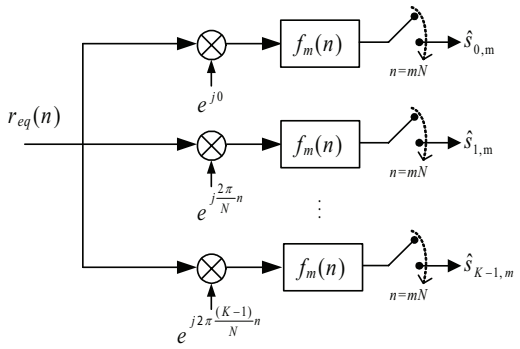

Fig. 5. Block diagram for Matched Filter Receiver.

C. Matched Filter Receiver with DSIC

From Figure 3 it is possible to observe that one of the major source of interference at the output of the MFR is the ICI among the adjacent subcarriers. This high ICI, which increases the BER, can be minimized by using the DSIC algorithm [29]. Figure 6 depicts the basic diagram of the DSIC.

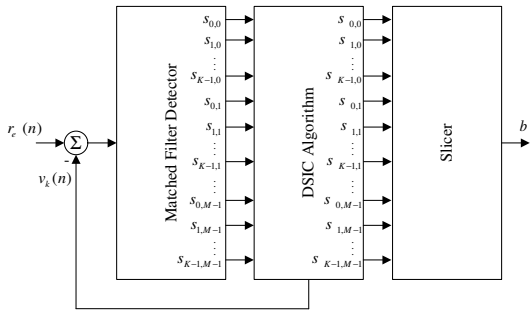

Fig. 6. Block diagram of a MF-DSIC detector.

The basic idea of this technique is to subtract the ICI caused by the $(k+1)$-th and $(k-1)$-th subcarriers from the signal received at the k-th subcarrier. First, the equalized received signal $\mathbf{r}_{\text{eq}}$ is applied to MFR, resulting in the ICI corrupted vector $\hat{\mathbf{s}}$. To eliminate the ICI from the signal received at the k-th subcarrier it will be necessary to use the $2M$ samples from $\hat{\mathbf{s}}$ corresponding to the data received at the $(k+1)$-th and $(k-1)$-th subcarriers in the M time-slots. A vector with $MN-1$ zeros is created and the samples in the positions corresponding to subcarriers k and $k+1$ for all time slots are updated with the associated samples from $\hat{\mathbf{s}}$. This procedure leads to

$$c(n) = \begin{cases} \hat{s}(n) & \text{if } n = k \pm 1 + mK, \quad m = 0, \ldots, M-1 \\ 0 & \text{otherwise} \end{cases} \tag{12}$$

The transmission matrix $\mathbf{A}$ can be used to generate a GFDM frame carrying the ICI information for the k-th subcarrier, i.e.,

$$\mathbf{v}_k = \mathbf{A}\mathbf{c} \tag{13}$$

where $\mathbf{v}_k$ is the GFDM frame with the ICI present for the k-th subcarrier and $\mathbf{c}$ is the vector representation of (12).

A new version of the equalized received signal is obtained by

$$\mathbf{r}'_{\mathbf{eq}} = \mathbf{r}_{\mathbf{eq}} - \mathbf{v}_{\mathbf{k}}, \tag{14}$$

which has low ICI in the k-th subcarrier.

The signal obtained in (14) is used to eliminate the ICI from the next subcarrier and the process continues until the ICI is mimimized from all subcarriers. The whole process can be iterated I times until the ICI reaches a desired level.

IV. SER Performance over Frequency-Selective Channels

OFDM is largely used in broadband communication systems because of its robustness against ISI and multipath fading. The symbol error rate (SER) of an OFDM system with J-QAM modulation over frequency-selective channels can be approximated by [30]

$$p_{e_s} \approx \frac{4(\sqrt{L}-1)}{\sqrt{2\pi L}\,K} \sum_{k=0}^{K-1} \frac{\gamma_k}{1+\gamma_k^2} \times e^{-\frac{\gamma_k^2}{2}}, \tag{15}$$

where

$$\gamma_k = \sqrt{|H_k|^2 \frac{3\bar{E}}{(L-1)\,N_0}}, \tag{16}$$

H_k is the channel gain in the frequency of the k-th subcarrier, $\bar{E}$ is the average energy of the QAM constellation and N_0 is the noise power spectral density.

In this paper, two selective channel delay profiles and an AWGN channel are considered. Table I shows the path gains, path delays and coherence bandwidth (correlation of 90%) for the selective channels. These channels can be used to model Wireless Regional Area Network (WRAN) environments [31].

Table II shows the system parameters used in SER simulations.

The CP length has been chosen to be larger than the maximum delay spread of the channel to assure that there is

TABLE I

DELAY PROFILE USED IN SIMULATIONS

Profile A	Coherence bandwidth: 7.23 kHz					
Delay (μs)	0	3	8	11	13	21
Path Gain (dB)	0	-7	-15	-22	-24	-19
Profile B	Coherence bandwidth: 11.97 kHz					
Delay (μs)	0	2	3	4	7	11
Path Gain (dB)	0	-7	-6	-22	-16	-20

TABLE II

SIMULATION PARAMETERS

Parameter	Value
Number of time-slots (M)	3
Number of subcarriers (K)	64
Upsampling Factor (N)	64
Duration of time-slot/OFDM symbol	256 μs
Subcarrier spacing	3,906 Hz
Constellation order (J)	4
Transmit Filter (GFDM)	Root Raised Cosine
Roll-off factor	0.5

no IFI. It is important to mention that the effect of the guard interval in the SNR has been compensated for.

Figures 7 to 9 show the SER for OFDM and GFDM. ZFR, MFR and MFR-DSIC with three iteractions has been considered for GFDM.

One possible conclusion based on the results observed is that the theoretical approximate curve utilized for OFDM can be used for GFDM analysis. The simulations results matches the theoretical curves in Figures 7 to 9. The MFR shows the poorer perfomance, since it is highly affected by ICI. The MFR-DSIC solves this problem, rendering the GFDM perfomance virtually equivalent to OFDM. The ZFR shows a performance gap when compared to MFR-DSIC of approximately 0.5 dB in high SNR for both channels.

In selective channels, the equalizer also presents a noise enhancement and, for lower values of SNR, this factor is more significative than the noise enhancement caused by the ZFR. This is observable by the proximity of the ZFR and MFR-DSIC curves in lower SNR. So, depending on the application, the MFR-DSIC may not justify its complexity gain when compared to ZFR.

V. CONCLUSIONS

GFDM is an interesting solution for CR networks because of its flexibility and spectral characteristics. The higher system complexity compared to OFDM can be justified by the benefits of lower out-of-band emissions, higher spectral efficiency and flexibility. This paper shows that equations currently used to model the OFDM behavior under selective channels can be used to model the GFDM behavior with MFR-DSIC when the channel can be considered flat for each subcarrier. And also shows that in applications where the typical SNR has lower values, the complexity gain of MFR-DSIC is not justifiable by its performance when compared to ZFR.

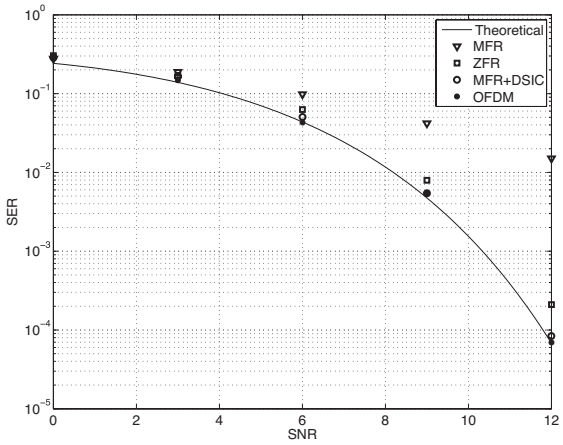

Fig. 7. SER for OFDM and GFDM over AWGN channel.

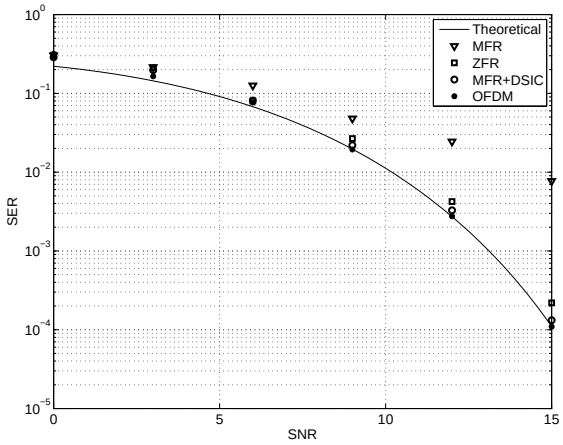

Fig. 8. SER for OFDM and GFDM over channel delay profile A.

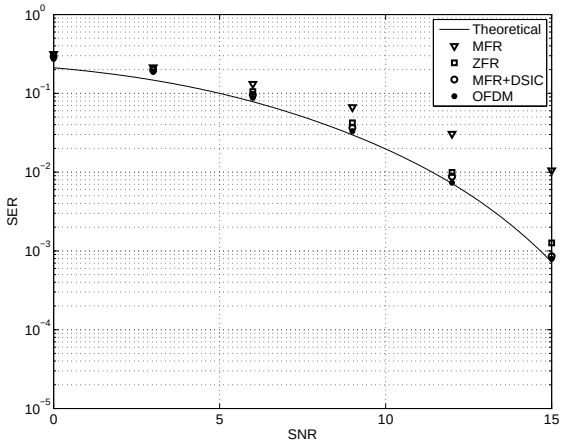

Fig. 9. SER for OFDM and GFDM over channel delay profile B.

ACKNOWLEDGMENTS

The authors would like to thank Inatel for the financial support and Dipl.-Ing. Nicola Michailow and Prof. Dr.-Ing. Dr. h.c. Gerhard Fettweis for the technical support.

REFERENCES

[1] Donald Cox. Fundamental Limitations on Increasing Data Rate in Wireless Systems. *IEEE Communications Magazine*, 46(12), December 2008.

[2] Kate Harrison, Shridhar Mubaraq Mishra, and Anant Sahai. How Much White-Space Capacity Is There? In *Proceedings of IEEE Symposium on New Frontiers in Dynamic Spectrum*, Singapore, April 2010.

[3] Hamid Reza Karimi. Geolocation Databases for White Space Devices in the UHF TV Bands: Specification of Maximum Permitted Emission Levels. In *Proceedings of IEEE Symposium on New Frontiers in Dynamic Spectrum Access Networks*, Aachen, Germany, May 2011.

[4] Peter Marshall. Analogue Switch-off and its Implications. In *Proceedings of the IEE Storage and Home Networks Seminar*, London, UK, November 2004.

[5] Francois Rancy, Elmar Zilles, and Jean-Jacques Guitot. Transition to digital TV and digital dividend. In *10th International Conference on Broadcasting Services (TELSIKS)*, Nis, Serbia, October 2011.

[6] Huseyin Arslan. *Cognitive Radio, Software Defined Radio, and Adaptive Wireless Systems*. Springer, [New York], 2007.

[7] Joseph Mitola. Cognitive Radio for Flexible Mobile Multimedia Communications. In *Proceeding of IEEE International Workshop on Mobile Multimedia Communications*, San Diego, CA, USA, November 1999.

[8] Carlos Cordeiro, Kiran Challapali, and Dagnachew Birru. IEEE 802.22: An Introduction to the First Wireless Standard based on Cognitive Radios. *Journal of Communications*, 1(1), 2006.

[9] 802.16h-2010. Technical report, Institute of Electrical and Electronics Engineers, New Jersey, USA, July 2010.

[10] Hyunduk Kang, Donghun Lee, Byung-Jang Jeong, and Allen C. Kim. Coexistence Between 802.22 and 802.11af over TV White Space. In *Proceedings of International Conference on ICT Convergence*, Seoul, South Korea, September 2011.

[11] Xinsheng Zhao, Zhiyi Guo, and Qiang Guo. A Cognitive Based Spectrum Sharing Scheme for LTE Advanced Systems. In *Proceedings of International Congress on Ultra Modern Telecommunications and Control Systems and Workshops*, Moscow, Russia, October 2010.

[12] Erik Axell, Geert Leus, Erik Larsson, and Vicent Poor. Spectrum Sensing for Cognitive Radio : State-of-the-Art and Recent Advances. *IEEE Signal Processing Magazine*, 29(3), May 2012.

[13] Amir Ghasemi and Elvino Sousa. Spectrum Sensing in Cognitive Radio Networks: Requirements, Challenges and Design Trade-offs. *IEEE Communications Magazine*, 46(4), April 2008.

[14] Yonghong Zeng, Ying-Chang Liang, Anh Tuan Hoang, and Rui Zhang. A Review on Spectrum Sensing for Cognitive Radio: Challenges and Solutions. *EURASIP Journal on Advances in Signal Processing*, January 2010.

[15] Ahmad Bahai and Burton Saltzberg. Kluwer Academic/Plenum, New York, 1999.

[16] Jaap Van De Beek and Fredrik Berggren. Out-of-Band Power Suppression in OFDM. *IEEE Communications Letters*, 12(9), September 2008.

[17] Myonghee Park, Heeyoung Jun, Jaehee Cho, Namshin Choand Daesik Hong, and Changeun Kang. PAPR reduction in OFDM transmission using hadamard transform. In *IEEE International Conference on Communications*, New Orleans, LA, USA, June 2000.

[18] Xin chun Wu, Jin xiang Wang, and Zhi gang Mao. A novel PTS Architecture for PAPR Reduction of OFDM Signals. In *2008 11th IEEE Singapore International Conference on Communication Systems*, Guangzhou, China, November 2008.

[19] Benjamin Lee, Dilip V. Sarwate, and Douglas L. Jones. Peak to Average Power Ratio Reduction of an OFDM Signal using a practical Selective Mapping Approach with Embedded Side-information. In *2009 Conference Record of the Forty-Third Asilomar Conference on Signals, Systems and Computers*, Pacific Grove, CA, USA, November 2009.

[20] Kyeongcheol Yang and S. Chang. Peak to Average Power Control in OFDM using standard arrays of Linear Block Codes. *IEEE Communications Letters*, 7(4), April 2003.

[21] Enrique Mariano Lizarraga, Alexis Alfredo Dowhuszko, and Victor Hugo Sauchelli. Improving Out-of-Band Power Emissions in OFDM Systems using Double-length Symbols. *IEEE Latin America Transactions*, 10(3), April 2012.

[22] Gerhard Fettweis, Marco Krondorf, and Steffen Bittner. GFDM - Generalized Frequency Division Multiplexing. In *IEEE 69th Vehicular Technology Conference*, Barcelona, Spain, April 2009.

[23] Nicola Michailow, Ivan Gaspar, Stefan Krone, Michael Lentmaier, and Gerhard Fettweis. Generalized Frequency Division Multiplexing: Analysis of an Alternative Multi-carrier Technique for Next Generation Cellular Systems. In *Proceedings of International Symposium on Wireless Communication Systems*, Paris, France, August 2012.

[24] Rohit Datta, Kamran Arshad, and Gerhard Fettweis. Analysis of Spectrum Sensing Characteristics for Cognitive Radio GFDM Signal. In *Proceedings of 8th International Wireless Communications and Mobile Computing Conference*, Limassol, Chipre, August 2012.

[25] Rohit Datta, Gerhard Fettweis, Yasunori Futatsugi, and Masayuki Ariyoshi. Comparative Analysis on Interference Suppressive Transmission Schemes for White Space Radio Access. In *Proceedings of IEEE 75th Vehicular Technology Conference (VTC Spring)*, Yokohama, Japan, May 2012.

[26] Nicola Michailow. *Integration of a GFDM Secondary System in an Existing OFDM System*. PhD thesis, Technische Universitat Dresden, Dresden, Germany, July 2010.

[27] Ahmad Bahai, Manonnet Singh, Andrea Goldsmith, and Burton Saltzberg. A New Approach for Evaluating Clipping Distortion in Multicarrier Systems. *IEEE Journal on Selected Areas in Communications*, 20(5), June 2002.

[28] Rohit Datta, Nicola Michailow, Michael Lentmaier, and Gerhard Fettweis. GFDM Interference Cancellation for Flexible Cognitive Radio PHY Design. In *Proceedings of the 76th IEEE Vehicular Technology Conference (VTC Fall'12)*, Quï¿½bec City, Canada, September 2012.

[29] Nicola Michailow, Rohit Datta, Štefan Krone, Michael Lentmaier, and Gerhard Fettweis. Generalized Frequency Division Multiplexing: A Flexible Multi-Carrier Modulation Scheme for 5th Generation Cellular Networks. In *Proceedings of the German Microwave Conference (GeMiC'12)*, Ilmenau, March 2012.

[30] Luciano Mendes and Renato Baldini Filho. Performance of WHT-STC-OFDM in Mobile Frequency Selective Channel. In *Proceedings of the International Telecommunication Symposium*, Manaus, 2010.

[31] Hyunwook Kim, Jaewoon Kim, Suckchel Yang, Minki Hong, and Yoan Shin. An effective mimo - ofdm system for ieee 802.22 wran channels. *IEEE Transactions on Circuits and Systems*, 55(8), August 2008.